Published in final edited form as:
Curr Biol. 2012 January 24; 22(2): 93–102. doi:10.1016/j.cub.2011.12.002.

Emergence of patterned activity in the developing zebrafish spinal cord

Erica Warp[1], **Gautam Agarwal**[1,2], **Claire Wyart**[3,4], **Drew Friedmann**[3], **Claire S. Oldfield**[1], **Alden Conner**[3], **Filippo Del Bene**[5,6], **Aristides B. Arrenberg**[5,7], **Herwig Baier**[5], and **Ehud Y. Isacoff**[1,3,8,#]

[1]Helen Wills Neuroscience Graduate Program, University of California, Berkeley, CA, USA

[3]Department of Molecular and Cell Biology, University of California, Berkeley, CA, USA

[5]Department of Physiology, Programs in Neuroscience, Genetics, and Developmental Biology, University of California, San Francisco, San Francisco, CA 94158-2722, USA

[8]Physical Bioscience Division, Lawrence Berkeley National Laboratory, Berkeley, California, USA

SUMMARY

Background—Developing neural networks display spontaneous and correlated rhythmic bursts of action potentials that are essential for circuit refinement. In the spinal cord, it is poorly understood how correlated activity is acquired and how its emergence relates to the formation of the spinal central pattern generator (CPG), the circuit that mediates rhythmic behaviors like walking and swimming. It is also unknown whether early, uncorrelated activity is necessary for the formation of the coordinated CPG.

Results—Time-lapse imaging in the intact zebrafish embryo with the genetically-encoded calcium indicator GCaMP3 revealed a rapid transition from slow, sporadic activity to fast, ipsilaterally correlated, and contralaterally anti-correlated activity, characteristic of the spinal CPG. Ipsilateral correlations were acquired through the coalescence of local microcircuits. Brief optical manipulation of activity with the light-driven pump Halorhodopsin revealed that the transition to correlated activity was associated with a strengthening of ipsilateral connections, likely mediated by gap junctions. Contralateral antagonism increased in strength at the same time. The transition to coordinated activity was disrupted by long-term optical inhibition of sporadic activity in motoneurons and VeLD interneurons, and resulted in more neurons exhibiting uncoordinated activity patterns at later time points.

Conclusions—These findings show that the CPG in the zebrafish spinal cord emerges directly from a sporadically active network as functional connectivity strengthens between local and then more distal neurons. These results also reveal that early, sporadic activity in a subset of ventral spinal neurons is required for the integration of maturing neurons into the coordinated CPG network.

[#]Address correspondence to ehud@berkeley.edu.
[2]Present address: Redwood Center for Theoretical Neuroscience, University of California, Berkeley, CA, USA
[4]Present address: Research Center of the Brain and Spine Institute (CRICM), Equipe ATIP/Avenir Inserm U975, CNRS, UMR 7225, Universite Pierre et Marie Curie UMP-S975, CHU Pitié-Salpêtrière - 75013 Paris, France
[6]Present address: Institut Curie, CNRS UMR3215, INSERM U934, 75724 Paris Cedex 05, France
[7]Present address: University of Freiburg, Freiburg, Germany

INTRODUCTION

Spontaneous activity is common to developing networks, occurring in the embryo during periods of concentrated axonal growth and synaptogenesis[1]. A hallmark of this activity is correlated population activity. Such correlations are hypothesized to guide the development of neural circuits[2], as demonstrated in the visual system where disruption of correlated retinal waves causes abnormal circuit development in downstream targets[3]. A transition from sporadic, cell-autonomous activity to correlated rhythmic activity has been observed in brain stem[4], cortex[5], and hippocampus[6], reflecting the emergence of connectivity and suggesting that early, sporadic activity may be necessary for the formation of more mature, correlated networks.

Early in the development of the motor system, cell-autonomous spontaneous calcium transients are observed in spinal cord neurons[7] before the maturation of the synaptic network. Later, spinal cord neurons display correlated patterns of spontaneous activity, beginning with bilaterally synchronized bursts of action potentials[8,9] that convert to alternation between the left and right sides when $GABA_A$ and glycine receptor signaling switches during development from depolarizing to hyperpolarizing[10]. In vertebrates, manipulation of correlated spontaneous activity in the spinal cord disrupts axon guidance[11], the balance between excitatory and inhibitory synaptic strength[12], and the formation of the central pattern generator (CPG)[13], which generates oscillatory rhythms for locomotion into adulthood[14]. Though cholinergic activity has been shown to be necessary for the maturation of rhythmic alternation between the two sides of the mammalian spinal cord[13], it is unknown if activity influences the acquisition of correlations on the same side of the cord and which cell types may mediate this activity-dependence.

We investigated the emergence of correlated patterns of spontaneous activity *in vivo* in the developing zebrafish spinal cord locomotor system using the genetically-encoded calcium indicator GCaMP3[15] to image spontaneous activity non-invasively at single-cell resolution in identified cells. The imaging identified a remarkably rapid transition from sporadic, uncorrelated activity to rhythms characteristic of the locomotor CPG with ipsilateral correlation and contralateral alternation. Acute optical manipulation of activity revealed that the development of functional connectivity underlies the emergence of the coordinated activity. Chronic optical inhibition of activity in motoneurons and VeLD interneurons early in the transition period disrupted the integration of maturing neurons into the correlated network, suggesting that the emergence of the coordinated CPG is activity-dependent.

RESULTS

Emergence of correlated activity

In vivo calcium imaging with genetically-encoded indicators has been used successfully to image neural activity in zebrafish embryos[16] and larvae[17,18]. We employed GCaMP3[15,18] for its high baseline fluorescence and high signal-to-noise ratio[15]. GCaMP3 and the light-gated inhibitory chloride pump Halorhodopsin (NpHR)[19,20], were targeted to neurons of interest using the *UAS/Gal4* system.

Spontaneous activity in the zebrafish spinal cord is restricted to ventral neurons of the motor system[21]. We used the *Gal4s1020t* line developed in an enhancer trap screen[22] to target a subset of these spontaneously active cells (Supplemental Fig. 1). We have previously characterized this line to contain primary and secondary motoneurons and Kolmer-Agduhr (KA) ascending interneurons in the spinal cord at 5 days post-fertilization (dpf)[23]. At 1 dpf, single cell imaging with BGUG[22] also revealed targeting to descending interneurons (Supplemental Fig. 1C, E). The *Gal4* insert for this line is near the *olig2* gene[23], which

exhibits an identical expression pattern and has been shown at 1 dpf to target motor neurons, KA cells, and ventral longitudinal descending (VeLD) interneurons, as well as BrdU-incorporating cells along the midline[24]. We therefore interpret the descending interneurons to be VeLDs.

Single cell electrophysiological recordings have identified three key neurons types—primary motoneurons, VeLD interneurons, and IC (ipsilateral caudal) descending interneurons—to be always active during spontaneous events in the zebrafish spinal cord at 20–24 hpf[21]. In the *Gal4s1020t* line we could image the population dynamics of spontaneous activity in primary motoneurons and VeLDs, two of the three key neuron types.

During embryonic development, zebrafish display spontaneous bursts of action potentials in the spinal cord that are associated with spontaneous contractions of the tail[25,26,21]. We imaged spontaneous calcium activity in *UAS:GCaMP3/Gal4s1020t* fish at 18 hpf, an hour after the onset of spontaneous behavior[25], and at 20 hpf, when electrophysiological correlation between pairs of spinal neurons has been previously observed[21], and when there is evidence for both electrical and chemical synapse formation in the zebrafish spinal cord[26,21]. Calcium imaging was performed on embryos paralyzed with ∝-bungarotoxin to eliminate spontaneous contractions, from a dorsal view to simultaneously observe cells on the left and right sides, and centered on somites 5 and 6. Spatial regions corresponding to single active neurons (e.g. regions outlined in Fig. 1A and D) and intensity traces over time (e.g. time series data in Fig. 1B and E) were extracted from movies using a semi-automated toolbox[27].

Though activity was present at 18 hpf, it was sporadic, with long-duration events (Fig. 1A–C, and Supplemental Movie 1) that were rarely associated with events in other ipsilateral cells and with no obvious relationship between the left and right sides of the cord. We did observe some correlation between ipsilateral cells at 18hpf, but this was just between small subsets of nearby cells (e.g. Fig. 1B, cells 1 & 2). In contrast, at 20 hpf events were shorter lasting, tightly correlated between nearly all ipsilateral cells, and organized in bursts of alternation between the left and right sides (Fig. 1D–F, and Supplemental Movie 2), as observed previously[16]. The left/right rhythmicity is reminiscent of activity patterns observed during swimming, but is significantly slower at this early coiling stage that precedes swimming[28]. We also observed fish that exhibited near-continual alternating bursts (Supplemental Fig. 1F).

Time-lapse calcium imaging was used to characterize the transition between the uncorrelated and correlated network states. Calcium imaging movies of 4-minute duration were taken every half hour between 17.5 and 21 hpf. To quantify changes in activity patterns, we calculated the correlation of GCaMP traces for all cell pairs in individual movies. Pair-wise correlation matrices of single cell traces in an example fish (Fig. 2A) showed little correlation at early time points and the few cell pairs that were correlated were weakly so. With time, correlations between ipsilateral neurons became stronger, while neurons on opposite sides of the cord became anti-correlated.

Pooled correlation data across fish showed that ipsilateral cells went from weak to strong correlation, reaching a maximum at 20 hpf, 3 hours after the onset of spontaneous behavior[25] (Fig. 2B, C). During this period, contralateral cells became increasingly anti-correlated (Fig. 2B, C). By 20 hpf rhythmic oscillations were apparent (Figs. 1F and 2B *right*), indicating that the components of a CPG are in place. Increases in ipsilateral correlation and decreases in event duration were detected in individual tracked cells that became active early (e.g. starting at 18 hpf, Supplemental Fig. 2A) as well as for cells that became active later (e.g. starting at 19.5 hpf, Supplemental Fig. 2B), suggesting that

maturation of the circuit involves the progressive addition of cells, each of which goes from an initial state of uncorrelated, slow activity to network-associated fast activity.

Ipsilateral synchronization through coalescence of local correlated groups

Spatiotemporal maps of correlated ensembles in most fish (6/9) at early stages showed multiple, non-overlapping correlated groups on the same side of the cord (Fig. 3, 18.5 hpf, left side). With time, the correlations between cells strengthened and the correlated groups increased in size, to eventually include virtually all ipsilateral cells in the field of view (Fig. 3, e.g. 20 hpf; and Supplemental Fig. 3A). Within these correlated ensembles, cells became more precisely time-locked (i.e. shorter lag times) during this early period of spontaneous activity (Supplemental Fig. 3B). In addition, event amplitude variability decreased during this period (Fig Supplemental Fig. 3C).

In younger embryos (17.5–18.5 hpf), the distance between cells participating in a synchronous event was relatively small, (i.e. correlations were seen between small numbers of neighboring cells), whereas temporally coupled cells covered a broader spatial region in older embryos (e.g. 20–21 hpf) (Supplemental Fig. 3D). Conversely, temporal spread was broad at younger stages, but tight at later stages as events became more accurately time-locked between ipsilateral cells (Supplemental Fig. 3D). Thus, ipsilateral correlation is accomplished through the coalescence of local correlated groups, which converts small events that are weakly correlated in small groups of cells into large events that occur synchronously on the entire side of the spinal cord. Although the zebrafish spinal cord develops in a rostral to caudal sequence[29], ipsilateral correlations do not emerge in a rostral/caudal pattern, at least in the region of cord that we imaged.

Increased functional connectivity accompanies emergence of correlated activity

Both chemical and electrical synapses have been implicated in mediating spontaneous activity in the spinal cord[9]. Paired recordings have shown that gap junctions play an essential role in the connectivity of the embryonic zebrafish spinal cord[21]. Additionally, uncoupling gap junctions with heptanol or by intracellular acidification eliminates spontaneous activity at 19–24hpf, while blockers of chemical transmission do not[26]. In older embryos (20–20.5 hpf), heptanol eliminated spontaneous activity in all but 3.7 ± 1.6% of cells (n=11 fish; see Supplemental Fig. 4B for example), whereas 34.7 ± 9.9% of cells remained active in younger embryos (17.5–18 hpf, n = 13 fish; P = 0.002, unpaired Student's *t* test; see Supplemental Fig. 4A for example). Though these results could be due to off target effects on calcium or potassium channels, they remain consistent with a model in which gap junctions are important for correlated activity at 20 hpf and younger neurons are more electrically cell-autonomous.

To examine this apparent emergence of functional connectivity between ipsilateral cells, we manipulated activity in single cells or in groups of cells and examined the effect on neighboring ipsilateral cells. We used the genetically-encoded light-driven chloride pump NpHR, which hyperpolarizes neurons in response to yellow light[19]. GCaMP3 and NpHR were genetically targeted to the same population of ventral spinal neurons in *Gal4s1020t/UAS:GCaMP3/UAS:NpHR-mCherry*[20] fish (Supplemental Fig. 5A). Spatial targeting of NpHR-activating light was accomplished using a digital micro mirror device (DMD). Its spatial resolution was tested by photoconversion of the fluorescent protein Kaede and light could be restricted to single cells (Supplemental Fig. 5E).

Since NpHR-activating 593nm light does not overlap with the excitation or emission spectrum of GCaMP3[15], calcium events could be imaged simultaneously during NpHR activation. Spontaneous calcium events imaged with GCaMP3 in NpHR-expressing fish

were blocked successfully by illumination of 593nm light at 19mW/mm^2 (Supplemental Fig. 5B–D). As seen earlier, including in other zebrafish neurons[19,20], light offset triggered rebound excitation (Supplemental Fig. 5C, D), allowing us to excite as well as inhibit with a single tool.

We observed striking differences in network responses to NpHR activation between younger and older embryos. Illumination of single cells in younger animals (18–18.5 hpf) caused robust inhibition in the illuminated cell and a rebound excitation upon light-off (Fig. 4A), but had no effect on other ipsilateral cells, suggesting low connectivity, where individual cells are functionally independent. In contrast, single cell illumination at 20–20.5 hpf did not significantly affect activity in either the illuminated cell or in other ipsilateral cells (Fig. 4B). However, illumination of a group of cells in a region encompassing two hemi-somites strongly suppressed activity during illumination and evoked rebound excitation upon light-off in both the illuminated cells and non-illuminated ipsilateral neighbors (Fig. 4C). Connectivity through electrical synapses can explain the ineffectiveness of NpHR single cell manipulation in the older embryo (Fig. 4B), as spread to neighbors of chloride current pumped in to an individual cell would reduce the efficacy of the hyperpolarization in that cell. The bi-directionality of electrical synapses can also explain why the inhibition and activation spread to non-illuminated cells in both the rostral and caudal directions (Fig. 4D) even though the only spontaneously active ipsilaterally projecting interneurons—the VeLD and IC cells—both have descending axons during this period of development[21,30,31]. In summary, our data suggest that increased functional connectivity underlies the emergence of ipsilateral correlation observed between 17.5 and 20 hpf (Fig. 2C).

Triggered rhythmic oscillation with NpHR reveals acquisition of contralateral antagonism

Supraspinal activation of the spinal CPG is bilateral for forward swimming, but triggers an alternating response in downstream spinal targets[32,28]. This behaviorally relevant coordinated firing relies on robust inhibitory connections between the two sides of the cord[14]. We tested whether the left and right sides of the cord were functionally antagonistic in the embryo by assessing network responses to bilateral stimulation evoked by NpHR rebound excitation that was confined to the neuronal cell types expressing in the *Gal4s1020t* line. *Gal4s1020t/UAS:GCaMP3/UAS:NpHR-mCherry* embryos were illuminated bilaterally over a four-somite region for 15 seconds, a duration that reliably triggered rebound excitation at light-off (Supplemental Fig. 5C, D and Fig. 5A, B). At 18 hpf, bilateral rebound activation triggered calcium events on the left and right sides of the cord with the initial wave of activity occurring nearly simultaneously on the two sides (Fig. 5A). In contrast, at 20 hpf the rebound excitation triggered a wave of activity first on one side and then, after a substantial delay, on the other side (Fig. 5B). The firing then alternated back and forth between the two sides, similar to what was seen in spontaneous locomotor-like activity (Fig. 1F and 2B *right*). The delay between correlated events (two or more cells participating) on the left and right sides following light offset increased significantly between 18 and 21 hpf ($P < 10^{-3}$, paired Student's *t* test, n = 6 fish; Fig. 5D), suggesting that contralateral antagonism is strengthened during this period.

Developmental transition disrupted by inhibition of activity

To determine the influence of uncorrelated spontaneous activity on the formation of the correlated network and the locomotor CPG, we inhibited spontaneous events for one hour with NpHR during the period of transition from uncorrelated to correlated activity (18 to 19 hpf), while imaging population activity with GCaMP3 (Fig. 6). To prevent cumulative desensitization of NpHR during long-term activation, we applied a 500 msec pulse of blue light (410 nm) every 10 seconds[33,19], concurrently with yellow light using a double bandpass filter to prevent rebound stimulation with yellow light-off (Fig. 6A). Light was

applied to the full imaged region covering both sides of the cord and approximately six somites, centered at somites 5 and 6.

Activation of NpHR from 18 to 19 hpf with yellow/blue light resulted in a reduction in the frequency of spontaneous events during the 18 to 19 hpf period in NpHR-positive fish as compared to three control groups: i) NpHR-negative fish without yellow/blue light, ii) NpHR-negative fish with yellow/blue light, and iii) NpHR-positive fish without yellow/blue light (Fig. 6B). NpHR-induced inhibition reduced activity by 66% initially (18 hpf) and by 53% by the end of the illumination period (19 hpf) compared to GCaMP only (group i) controls (Fig, 6B). An intermediate decrease in the frequency of spontaneous events was observed in NpHR-positive fish that did not receive the yellow/blue light protocol (group iii). This effect was attributed to the fact that the 488 nm imaging light overlaps with the NpHR excitation spectrum and activates the pump by approximately 18%[19]. To eliminate potential effects of the imaging light on the frequency of spontaneous events, we imaged the population patterns only at the end of the experiment (22 hpf) for NpHR without yellow/blue light controls.

We observed a substantial reduction in pair-wise ipsilateral correlation in the experimental fish (NpHR-positive fish receiving the yellow/blue light protocol) when compared to controls (Fig. 6C), though the four groups did not differ at baseline at 18 hpf (ipsilateral correlation one-way ANOVA, $P = 0.22$). This reduction in correlation became evident at 20.5 hpf and continued through 22 hpf (Fig. 6C). Additionally, the three controls were similar at 22 hpf, indicating that neither NpHR expression alone, possible NpHR constitutive activity alone, nor yellow/blue light alone disrupts the emergence of correlated activity.

An examination of the activity in control and experimental fish showed that by 22 hpf the experimental fish had a larger proportion of active cells with immature phenotypes (Fig. 7B). As shown above (Figs. 1–3) and in control fish (Fig. 7A), most active cells were part of an ipsilateral, correlated network in the older embryo, with a small minority of the cells showing long-duration, uncorrelated events and usually residing more medially in the spinal cord (Fig. 1D, E and Fig. 7A, *asterisks*). In contrast, in experimental fish approximately 50% of the active cells were uncorrelated, with long-duration events (Fig. 7B, *asterisks*; and Fig. 7C), displaying the more immature activity pattern that we observed in our single-cell tracking (Supplemental Fig. 2). Associated with this perturbed pattern of activity, we found that in the experimental animals a larger fraction of the active cells were located closer to the midline of the spinal cord (Fig. 7B, *asterisks*; and Fig. 7D), where more immature cells, like BrdU-incorporating progenitor cells, have been shown to reside[24]. Groups did not differ in events kinetics (width at half maximum one-way ANOVA, $P = 0.30$) nor the location of active cells (distance to midline one-way ANOVA, $P = 0.28$) at 18 hpf before activity manipulation. The number of active cells per field of view was not significantly different between experimental and control fish (Supplemental Fig. 6), suggesting that the optical inhibition of activity in motoneurons and VeLDs perturbed the developmental transition by reducing the efficiency with which cells that originated at the midline joined the lateral correlated network.

DISCUSSION

Rapid emergence of ipsilateral correlation

Optical measurements of spontaneous activity in genetically selected ventral spinal neurons in live zebrafish revealed a rapid transition from uncorrelated, sporadic slow activity to ipsilaterally correlated fast activity. The transition to correlated activity could be accounted for by the formation of electrical connections, which initially couple nearby neurons into

local microcircuits and then merge to include the majority of active ipsilateral neurons into a single coupled network.

Our observations *in vivo* are consistent with observations made previously. In Xenopus, cell-autonomous calcium events are seen in dissociated spinal cultures and in the isolated spinal cord, with short duration calcium events becoming correlated between small groups of neurons later in development[7]. In isolated spinal cord of rodent[34] and chick[35], spontaneous events, which are correlated between motoneurons and interneurons, propagate between multiple spinal segments[35]. In the zebrafish spinal cord, cell-autonomous calcium events have been detected in axon-less cells of the 19–26 hpf embryo in imaging experiments, but likely overlap minimally with the events we detected due to their very slow kinetics[36]. Correlated depolarizations have been observed between pairs of ventral neurons in dual-cell electrophysiological recordings in 20–24 hpf zebrafish embryos[21], which likely correspond to the correlated calcium events we observed with GCaMP. During swimming, waves of activity propagate down the ipsilateral spinal cord, resulting in nearby motoneurons being more correlated than distant ones[14,28]. A similar, though slower, rostral to caudal propagation is observed in spontaneously active motoneurons of 24 hpf zebrafish embryos[16]. We observed that nearby spinal neurons became correlated before distant neurons, suggesting more mature rostral/caudal relationships are established as the first connections are formed between neurons.

The changes in global activity patterns that we observed were associated with a rapid strengthening of functional connectivity between ipsilateral neurons, as seen from the change in the spread of NpHR inhibition and rebound excitation to non-illuminated cells, suggesting that early activity is cell-autonomous and later activity depends on network interactions. The initiation of rhythmic spontaneous events in the rodent and chick spinal cord has been shown to depend on recurrent excitation between GABA-, glycine- and glutamatergic interneurons and cholinergic motoneurons[1,9]. The ipsilateral network interactions that we observed in the zebrafish appear to be mediated via electrical synapses, as shown in previous studies[26,21], though chemical synapses may also play a role. Gap junctions also appear to play an integral role in the propagation of correlated spontaneous activity in the spinal cord of rodents[9] and chicks[37], and appear to form some of the first connection in the developing retina[38], cortex[39] and hippocampus[6].

Contralateral antagonism emerges concurrently with ipsilateral correlation

We found that as the coupled ipsilateral network was established there also emerged a superstructure in which the spontaneous activity alternated from side-to-side, a fundamental characteristic of the CPG, which has been shown to involve contralateral inhibition through chemical synapses[14]. Earlier lesion studies have indicated that spontaneous activity and left/right alternation in the spinal cord of embryonic zebrafish does not rely on input from the brain[25,40], suggesting the network mediating this rhythmic activity is endogenous to the spinal cord. Given that, among the cells expressing in our Gal4 line, only KAs and VeLDs project within the spinal cord, and, of these, only the VeLDs are active in the first day of development, it therefore appears that the VeLDs, and neurons that they drive, can account for a minimal circuit for locomotor-like activity and behavior.

In rats and mice, spontaneous events are at first synchronized between both sides of the spinal cord, becoming alternating around birth when the activation of $GABA_A$ and glycine receptors become hyperpolarizing[8,9]. We did not observe a period of synchronized spontaneous events between the left and right sides of the spinal cord in the zebrafish. Rather, the first coordinated patterns consisted of both ipsilateral correlation and contralateral alternation (Fig. 2B, C). We observed similar patterns of alternating activity with bilateral rebound-activation with NpHR. The similarity between spontaneous and

NpHR rebound-evoked alternation suggests that a bilateral drive may be responsible for triggering the earliest alternating bursts of locomotor-like activity in the embryonic zebrafish.

Activity-dependent emergence of the CPG

Inhibition of activity for one hour with NpHR during the transition from sporadic to patterned activity disrupted the emergence of correlated, short duration, rhythmic activity, indicating that early activity is either instructive or permissive for the maturation of the spinal network. In the normal development of the spinal cord, our imaging revealed that cells first display long-duration, uncorrelated events before transitioning to brief, correlated activity as they establish functional connectivity with other neurons. This transition occurred in neurons that became active early (e.g. Supplemental Fig. 2A) and in neurons that matured and integrated into the network at a later stage (e.g. Supplemental Fig. 2B). Light-driven reduction of activity with NpHR reduced the overall ipsilateral correlation by reducing the fraction of cells that made the transition to brief, correlated activity. As seen in control fish experiencing normal activity, the uncorrelated cells tended to be located more medially in the spinal cord, except that in the fish whose activity had been inhibited by light they went from being a small minority to being roughly half of the active cells (Fig. 7).

These effects are striking given that the inhibition of activity is only by approximately half, that it lasts for only one of the three hours of the developmental transition and that it occurs in only a subset of ventral spinal neurons: the VeLD interneurons and motoneurons (the KAs, also targeted in the *Gal4s1020t* line, have not been shown to display rhythmic spontaneous activity[21]). These observations imply that early spontaneous activity in VeLD interneurons and/or motoneurons, or in neurons that they drive, is required for the integration of less mature neurons into the correlated network and for the acquisition of normal patterns of population activity. The effect that we observe from inhibiting activity between 18 and 19 hpf was not present until 20.5 hpf, suggesting that inhibition of activity in the few cells that are active early likely alters the integration of other neurons that mature later.

Previous studies have shown that calcium fluctuations play an essential role in developmental processes such as cell migration[41], axon guidance[42] and the expression of the membrane proteins that control cell excitability[43]. It is possible that some or all of these mechanisms underlie the effect of activity manipulation that we observe. For example, a lateral position could be required for integration into the correlated network and blocking migration to this position could subsequently reduce the number of coupled cells. It has recently been shown that endogenous patterns of spontaneous activity are required for the proper development of coordinated patterns of activity in the motor system of an invertebrate[44]. Here we show that early uncorrelated spontaneous activity is required for the formation of coordinated motor circuits in a vertebrate.

Conclusion

Correlated, rhythmic spontaneous activity is a common feature of developing networks and is essential for normal circuit maturation. Applying non-invasive optical tools to image activity we observed a rapid transition from sporadic, long-duration, uncorrelated activity to fast, correlated, and rhythmic spontaneous activity in the spinal cord of the intact developing zebrafish. Correlated activity between neurons on the same side of the cord was found to emerge through the formation of small local microcircuits and their subsequent coalescence into a single ipsilateral network, at the same time as side to side alternation emerged. This transition to patterned locomotor-like population activity is perturbed by optical inhibition of motoneurons and VeLD interneurons during the transition period, impeding the integration

of maturing neurons into the coordinated network. These results indicate that the formation of the spinal CPG is dependent on activity that occurs before functional connectivity is robustly established in the network.

EXPERIMENTAL PROCEDURES

The following transgenic lines were used for experiments (naming according to official zebrasfish nomenclature): *Et(-0.6hsp70l:Gal4-VP16)s1020t* (a.k.a. *Gal4s1020t*)[22]; *Tg(UAS-E1b:Kaede)s1999t/+* (a.k.a. *UAS:Kaede*)[22]; and *Tg(UAS:NpHR-mCherry)s1989t* (a.k.a. *UAS:NpHR)*[20], *as well as UAS:GCaMP3*[18].

Imaging, photomanipulation and analysis methods described in the Supplement.

Supplementary Material

Refer to Web version on PubMed Central for supplementary material.

Acknowledgments

We thank K. McDaniel, W. Staub, J. Saint-Hillaire and D. Weinman for fish care; K. McDaniel for assistance with experiment set-up; M. Feller for critical reading of the manuscript, and H. Aaron and Intelligent Imaging Innovations for advice and assistance with the optical system. Support for the work was provided by the National Institutes of Health Nanomedicine Development Center for the Optical Control of Biological Function, PN2EY018241 (E.Y.I.), the Human Frontier Science Program, RGP0013/2010 (E.Y.I.), the National Science Foundation (FIBR 0623527 (E.Y.I.), and the National Institute of Health NRSA fellowship (E.W.).

References

1. Blankenship AG, Feller MB. Mechanisms underlying spontaneous patterned activity in developing neural circuits. Nat Rev Neurosci. 2010; 11:18–29. [PubMed: 19953103]
2. Spitzer NC. Coincidence detection enhances appropriate wiring of the nervous system. Proc Natl Acad Sci USA. 2004; 101:5311–5312. [PubMed: 15067118]
3. Torborg CL, Feller MB. Spontaneous patterned retinal activity and the refinement of retinal projections. Prog Neurobiol. 2005; 76:213–235. [PubMed: 16280194]
4. Gust J, Wright JJ, Pratt EB, Bosma MM. Development of synchronized activity of cranial motor neurons in the segmented embryonic mouse hindbrain. J Physiol (Lond). 2003; 550:123–133. [PubMed: 12730346]
5. Corlew R, Bosma MM, Moody WJ. Spontaneous, synchronous electrical activity in neonatal mouse cortical neurones. J Physiol (Lond). 2004; 560:377–390. [PubMed: 15297578]
6. Crépel V, et al. A parturition-associated nonsynaptic coherent activity pattern in the developing hippocampus. Neuron. 2007; 54:105–120. [PubMed: 17408581]
7. Gu X, Olson EC, Spitzer NC. Spontaneous neuronal calcium spikes and waves during early differentiation. J Neurosci. 1994; 14:6325–6335. [PubMed: 7965039]
8. Nakayama K, Nishimaru H, Kudo N. Basis of changes in left-right coordination of rhythmic motor activity during development in the rat spinal cord. J Neurosci. 2002; 22:10388–10398. [PubMed: 12451138]
9. Hanson MG, Landmesser LT. Characterization of the circuits that generate spontaneous episodes of activity in the early embryonic mouse spinal cord. J Neurosci. 2003; 23:587–600. [PubMed: 12533619]
10. Delpy A, Allain AE, Meyrand P, Branchereau P. NKCC1 cotransporter inactivation underlies embryonic development of chloride-mediated inhibition in mouse spinal motoneuron. J Physiol (Lond). 2008; 586:1059–1075. [PubMed: 18096599]
11. Hanson MG, Milner LD, Landmesser LT. Spontaneous rhythmic activity in early chick spinal cord influences distinct motor axon pathfinding decisions. Brain Res Rev. 2008; 57:77–85. [PubMed: 17920131]

12. Gonzalez-Islas C, Wenner P. Spontaneous network activity in the embryonic spinal cord regulates AMPAergic and GABAergic synaptic strength. Neuron. 2006; 49:563–575. [PubMed: 16476665]
13. Myers CP, et al. Cholinergic input is required during embryonic development to mediate proper assembly of spinal locomotor circuits. Neuron. 2005; 46:37–49. [PubMed: 15820692]
14. Grillner S. Biological pattern generation: the cellular and computational logic of networks in motion. Neuron. 2006; 52:751–766. [PubMed: 17145498]
15. Tian L, et al. Imaging neural activity in worms, flies and mice with improved GCaMP calcium indicators. Nat Methods. 2009; 6:875–881. [PubMed: 19898485]
16. Muto A, et al. Genetic visualization with an improved GCaMP calcium indicator reveals spatiotemporal activation of the spinal motor neurons in zebrafish. Proc Natl Acad Sci USA. 2011; 108:5425–5430. [PubMed: 21383146]
17. Higashijima, S-ichi; Masino, MA.; Mandel, G.; Fetcho, JR. Imaging neuronal activity during zebrafish behavior with a genetically encoded calcium indicator. J Neurophysiol. 2003; 90:3986–3997. [PubMed: 12930818]
18. Del Bene F, et al. Filtering of Visual Information in the Tectum by an Identified Neural Circuit. Science. 2010; 330:669–673. [PubMed: 21030657]
19. Zhang F, et al. Multimodal fast optical interrogation of neural circuitry. Nature. 2007; 446:633–639. [PubMed: 17410168]
20. Arrenberg AB, Del Bene F, Baier H. Optical control of zebrafish behavior with halorhodopsin. Proc Natl Acad Sci USA. 2009; 106:17968–17973. [PubMed: 19805086]
21. Saint-Amant L, Drapeau P. Synchronization of an embryonic network of identified spinal interneurons solely by electrical coupling. Neuron. 2001; 31:1035–1046. [PubMed: 11580902]
22. Scott EK, et al. Targeting neural circuitry in zebrafish using GAL4 enhancer trapping. Nat Methods. 2007; 4:323–326. [PubMed: 17369834]
23. Wyart C, et al. Optogenetic dissection of a behavioural module in the vertebrate spinal cord. Nature. 2009; 461:407–410. [PubMed: 19759620]
24. Park HC, Shin J, Appel B. Spatial and temporal regulation of ventral spinal cord precursor specification by Hedgehog signaling. Development. 2004; 131:5959–5969. [PubMed: 15539490]
25. Saint-Amant L, Drapeau P. Time course of the development of motor behaviors in the zebrafish embryo. J Neurobiol. 1998; 37:622–632. [PubMed: 9858263]
26. Saint-Amant L, Drapeau P. Motoneuron activity patterns related to the earliest behavior of the zebrafish embryo. J Neurosci. 2000; 20:3964–3972. [PubMed: 10818131]
27. Mukamel EA, Nimmerjahn A, Schnitzer MJ. Automated analysis of cellular signals from large-scale calcium imaging data. Neuron. 2009; 63:747–760. [PubMed: 19778505]
28. Masino MA, Fetcho JR. Fictive swimming motor patterns in wild type and mutant larval zebrafish. J Neurophysiol. 2005; 93:3177–3188. [PubMed: 15673549]
29. Kimmel CB, Ballard WW, Kimmel SR, Ullmann B, Schilling TF. Stages of embryonic development of the zebrafish. Dev Dyn. 1995; 203:253–310. [PubMed: 8589427]
30. Bernhardt RR, Chitnis AB, Lindamer L, Kuwada JY. Identification of spinal neurons in the embryonic and larval zebrafish. J Comp Neurol. 1990; 302:603–616. [PubMed: 1702120]
31. Kuwada JY, Bernhardt RR. Axonal outgrowth by identified neurons in the spinal cord of zebrafish embryos. Exp Neurol. 1990; 109:29–34. [PubMed: 2192908]
32. Deliagina TG, Zelenin PV, Orlovsky GN. Encoding and decoding of reticulospinal commands. Brain Res Brain Res Rev. 2002; 40:166–177. [PubMed: 12589915]
33. Hegemann P, Oesterhelt D, Bamberg E. The transport activity of the light-driven chloride pump halorhodopsin is regulated by green and blue light. Biochimica et Biophysica Acta (BBA) - Biomembranes. 1985; 819:195–205.
34. Ren J, Greer JJ. Ontogeny of rhythmic motor patterns generated in the embryonic rat spinal cord. J Neurophysiol. 2003; 89:1187–1195. [PubMed: 12626606]
35. O'Donovan M, Ho S, Yee W. Calcium imaging of rhythmic network activity in the developing spinal cord of the chick embryo. J Neurosci. 1994; 14:6354–6369. [PubMed: 7965041]
36. Ashworth R, Bolsover SR. Spontaneous activity-independent intracellular calcium signals in the developing spinal cord of the zebrafish embryo. Brain Res Dev Brain Res. 2002; 139:131–137.

37. Milner LD, Landmesser LT. Cholinergic and GABAergic inputs drive patterned spontaneous motoneuron activity before target contact. J Neurosci. 1999; 19:3007–3022. [PubMed: 10191318]
38. Syed MM, Lee S, Zheng J, Zhou ZJ. Stage-dependent dynamics and modulation of spontaneous waves in the developing rabbit retina. J Physiol (Lond). 2004; 560:533–549. [PubMed: 15308679]
39. Yuste R, Peinado A, Katz LC. Neuronal domains in developing neocortex. Science. 1992; 257:665–669. [PubMed: 1496379]
40. Downes GB, Granato M. Supraspinal input is dispensable to generate glycine-mediated locomotive behaviors in the zebrafish embryo. J Neurobiol. 2006; 66:437–451. [PubMed: 16470684]
41. Komuro H, Rakic P. Intracellular Ca2+ fluctuations modulate the rate of neuronal migration. Neuron. 1996; 17:275–285. [PubMed: 8780651]
42. Gu X, Spitzer NC. Distinct aspects of neuronal differentiation encoded by frequency of spontaneous Ca2+ transients. Nature. 1995; 375:784–787. [PubMed: 7596410]
43. Desarmenien MG, Spitzer NC. Role of calcium and protein kinase C in development of the delayed rectifier potassium current in Xenopus spinal neurons. Neuron. 1991; 7:797–805. [PubMed: 1742026]
44. Crisp SJ, Evers JF, Bate M. Endogenous patterns of activity are required for the maturation of a motor network. J Neurosci. 2011; 31:10445–10450. [PubMed: 21775590]

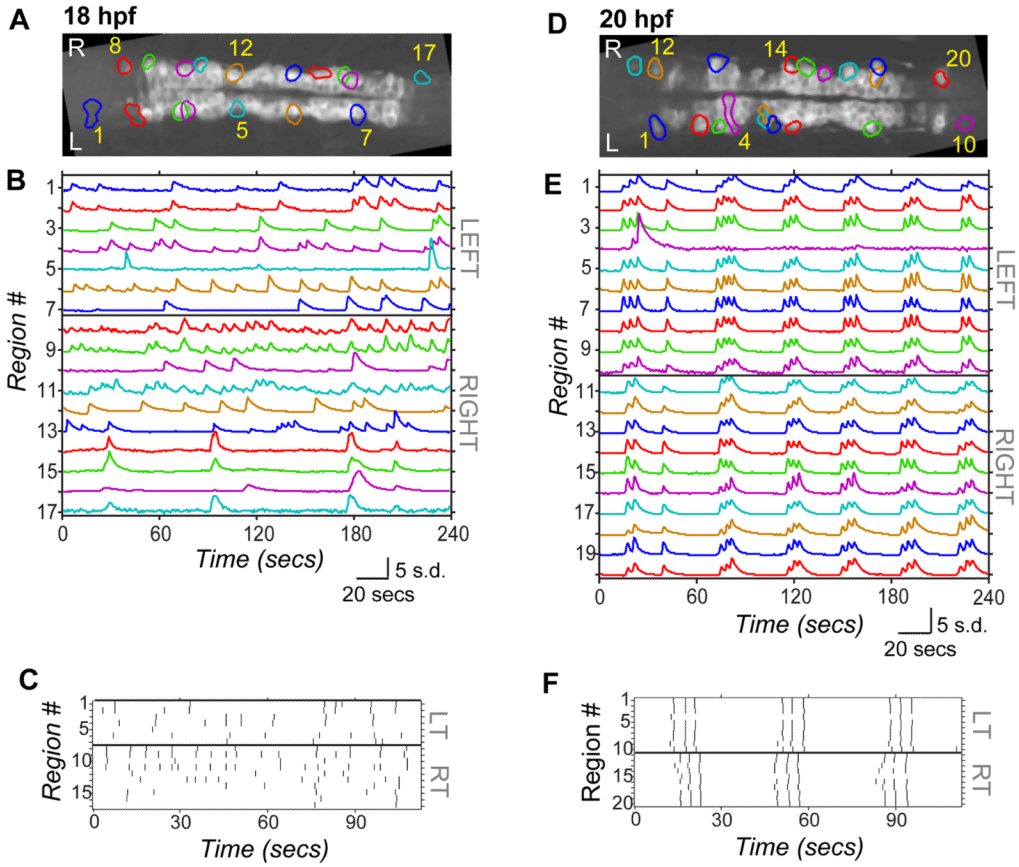

Figure 1. Spontaneous calcium activity in spinal neurons progresses from sporadic to locomotor-like during embryonic development

GCaMP3 activity in single neurons in one example embryo at 18 hpf (left) and 20 hpf (right). (A,D) Dorsal views of GCaMP3 baseline fluorescence with active regions circled (rostral left; imaged area somites 4–8). (B,E) Normalized intensity traces for active regions (identified on y-axis) for the left and right sides of the cord, with amplitude corresponding to standard deviations (s.d.) of fluorescence away from baseline. At 18 hpf (B) ipsilateral neurons have little correlated firing, though some synchronization is observed (e.g. cells 8 & 9). At 20 hpf (E) ipsilateral neurons are tightly synchronized, with few exceptions (e.g. cell 4; note elongated shape extending to the midline). (C,F) Raster plots of detected events for subsection of data in (B) and (E). At 18 hpf (C), population activity is uncoordinated. By 20 hpf (F), ipsilateral cells are synchronized, contralateral cells alternate, and a higher order left/right bursting organization is observed. See also Supplemental Fig. 1.

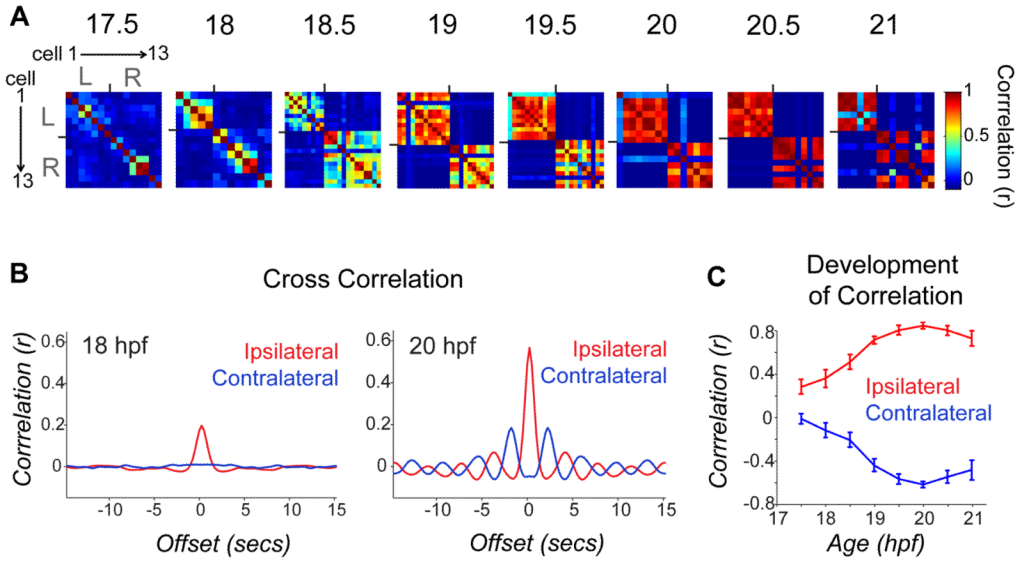

Figure 2. Pair-wise cell relationships progress from independent to ipsi-correlated/contra-anti-correlated during a short period of development

(A) Correlation matrices of single cell traces through the development of an example embryo. Each pixel represents a pair-wise comparison between 2 cells, with high correlation values in red and perfect auto-correlation along the diagonal. Cells are sorted left to right and top to bottom as shown for 17.5 hpf. Ticks mark border between left and right cord and bound a high degree of ipsilateral correlation observed at later time points. (B) Cross-correlation shows a strengthening of ipsilateral coupling between 18 and 20 hpf and acquisition of oscillatory rhythm by 20 hpf. Cross-correlation was calculated by averaging time-shifted correlation data for all ipsilateral and contralateral cell pairs in individual movies, pooled across 9 different fish. (C) Average pair-wise correlations for synchronous events comparing ipsilateral and contralateral cell pairs from individual time lapse movies acquired from fish ages 17.5 to 21 hpf and pooled across fish. We observed a significant difference between ipsilateral correlations in younger versus older embryos (18 hpf, r = 0.272 ± 0.082; 20 hpf, r = 0.761 ± 0.031; $P < 10^{-3}$, paired Student's *t* test; n = 9 fish), and a significant increase in the anti-correlation of contralateral cells (18 hpf, r = −0.207 ± 0.067; 20 hpf, r = −0.710 ± 0.028; $P = < 10^{-3}$, paired Student's *t* test; n = 9 fish). n=9 fish for 18–21 hpf; n=4 fish at 17.5 hpf. Error bars=s.e.m. See also Supplemental Fig. 2.

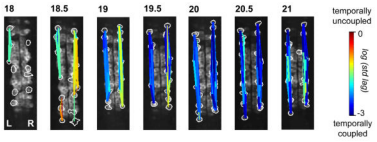

Figure 3. Ipsilateral correlation is acquired through the progressive synchronization of local subgroups of cells

Spatial maps of correlated groups in an example fish from 18 to 21 hpf show small local circuits containing a few cells at 18 and 18.5 hpf that expand into full correlation of each side at later stages. Correlations between all cell pairs were calculated and lines were drawn between cell pairs with correlations greater than 0.2, with thicker lines representing stronger correlation. Line color represents the log of the standard deviation of the lags between event start times of cell pairs and shows an overall increase in temporal precision between ipsilateral pairs as development progresses. See also Supplemental Fig. 3.

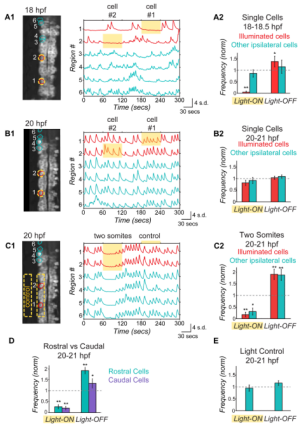

Figure 4. Optical manipulation of targeted network components with NpHR reveals changes in functional connectivity between ipsilateral neurons during development

(A,B) Single cell optical manipulation of spontaneous activity with NpHR at 18 hpf (A) and 20 hpf (B). 593nm light at 19mW/mm^2 is targeted successively to two regions outlined in yellow (A1, *left*), while calcium population activity is simultaneously recorded (A1, *right*) in the illuminated cells (red) and in the other ipsilateral cells (teal), and here displayed as normalized traces (standard deviation, s.d.) with regions indicated on y-axis. (A1) At 18 hpf, application of yellow light to a single cell (during yellow highlight bar) inhibits only the illuminated cell, while other cells remain active. (A2) Pooled results (n=6 embryos) show inhibition during light-ON and activation at light-OFF to be limited to illuminated cells (red bars). (B) At 20 hpf, single cell illumination has no effect on activity of either the illuminated or non-illuminated cells (n=7 embryos). (C) At 20 hpf, illumination of one side of spinal cord in region spanning two somites (yellow outline in image, *left*) inhibits and rebound excites both the illuminated cells and other ipsilateral cells (n=7 embryos). (D) Reduction of activity and rebound due to NpHR activation at 20 hpf are observed in cells that are both rostral and caudal to the region illuminated. (E) Control application of light aimed to the side of the cord but within the embryo (C1) does not perturb activity (n=7 embryos), indicating that effect on un-illuminated ipsilateral cells is not due to light scattering though we acknowledge light scattering may have different properties in this region. Rostral, up in fluorescence images; * P<0.05; ** P<0.01, paired Student's *t* test. See also Supplemental Figs. 4 and 5.

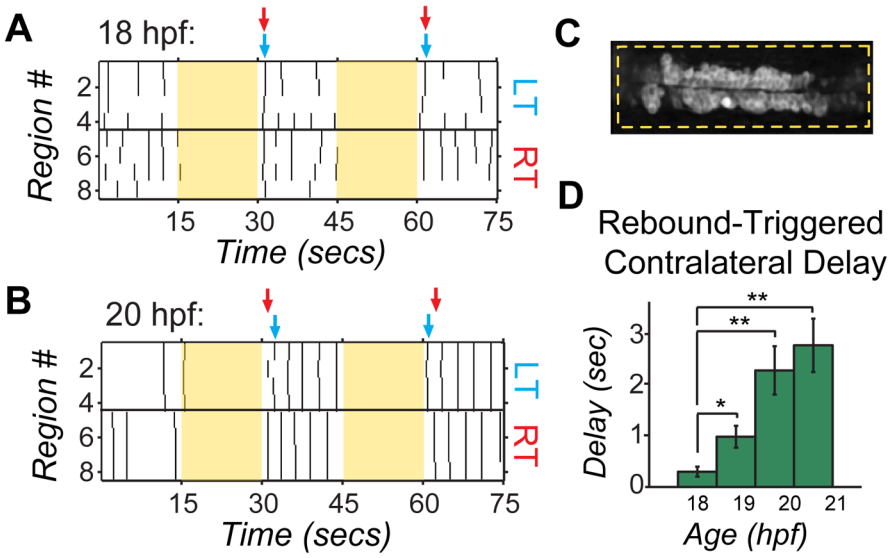

Figure 5. Bilateral activation with NpHR rebound reveals acquisition of contralateral antagonism during development

Raster plots of spontaneous events of left and right cells in a single embryo at 18 hpf (A) and 20 hpf (B) during and following bilateral NpHR inhibition with 593nm light (yellow bars) covering approximately four somites (C). (A) Bilateral activation following NpHR inhibition at 18 hpf results in near simultaneous activation of left (LT) and right (RT) cells following light offset. Arrows indicate the time when two or more cells participate in an event following light offset for one side of the cord (left side, blue; right side, red). (B) At 20 hpf, activation at light offset of bilateral illumination results in a burst of activity in which one side fires first, followed, after a delay, by firing on the other side and continuing in alternation of firing from side to side. In this example, the right side is active first in trial #1, but the left side is active first in the trial #2. (D) The delay following offset of bilateral illumination between synchronous events on the left and right sides of the cord (two or more cells participating) increases during development, suggesting an increase in left/right antagonism. n = 5 fish (4 trials per fish per condition); * P<0.05; ** P<0.01, paired Student's *t* test. See also Supplemental Fig. 5.

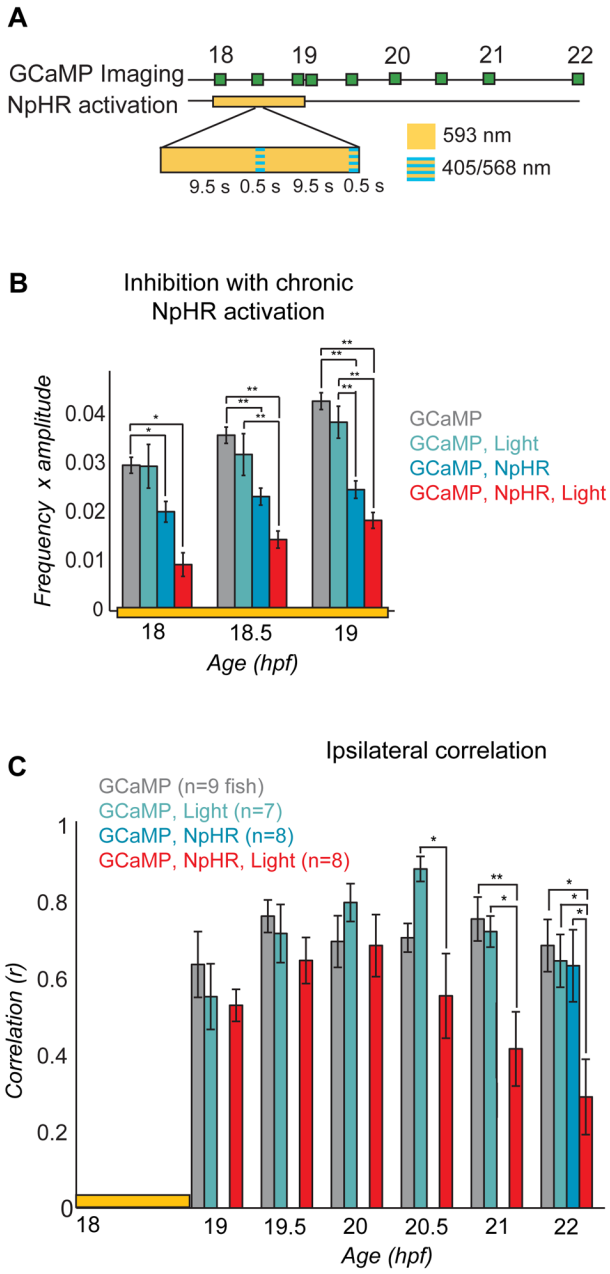

Figure 6. Inhibition of spontaneous events with NpHR from 18 to 19 hpf yields a subsequent decrease in ipsilateral correlation

(A) Experimental protocol for chronic inhibition experiments. GCaMP movies were acquired during the light manipulation (at 18, 18.5 and 19 hpf) with 488 nm light to determine the effectiveness of the light protocol, and at half hour/hour intervals thereafter (until 22 hpf) to asses subsequent changes in network dynamics. Stimulation of NpHR was performed from 18 to 19 hpf with continuous 593 nm light at 19nW/mm^2 interspersed every 10 seconds with 500 msec long pulses of light simultaneously at two wavelengths: 405 nm to reduce desensitization of the NpHR and 568 nm to activate it. (B) The frequency of calcium events from 18 to 19 hpf was quantified for experimental fish expressing NpHR and receiving the yellow light protocol (GCaMP, NpHR, Light) as well as for three kinds of control fish: i) NpHR-negative fish without yellow/blue light (GCaMP), ii) NpHR-negative

fish with yellow/blue light (GCaMP, Light), and iii) NpHR-positive fish without yellow/blue light (GCaMP, NpHR). Means were calculated per cell, n = 13–385 cells per group. There was a significant effect of group at 18, 18.5 and 19 hpf (one-way ANOVA at each time point, $P<0.05$), with greatest decreases in the experimental group (red bars; GCaMP, NpHR, Light). The reduction in activity in embryos that expressed NpHR but did not receive the light protocol can be attributed to the activation of NpHR by the 488 nm imaging light. (C) Average ipsilateral pair-wise correlations measured for experimental fish (n = 8) and the three control groups (n = 7 to 9) in movies acquired after the termination of the yellow/blue light protocol reveal a decrease in correlated activity in the experimental fish (GCaMP, NpHR, Light) at later time points compared to all of the controls. There was no difference between groups at 19, 19.5 and 20 hpf (one-way ANOVA at each time point, $P>0.05$), with significant differences at 20.5, 21 and 22 hpf (one-way ANOVA at each time point, $P<0.05$). Note that to avoid activation of NpHR in controls without yellow/blue light protocol, GCaMP imaging in this group was only done at 22 hpf. Bars=s.e.m. Asterisks in (B) and (C) mark pair-wise significance from post-hoc comparison with Bonferroni correction (* $P<0.05$; ** $P<0.01$)

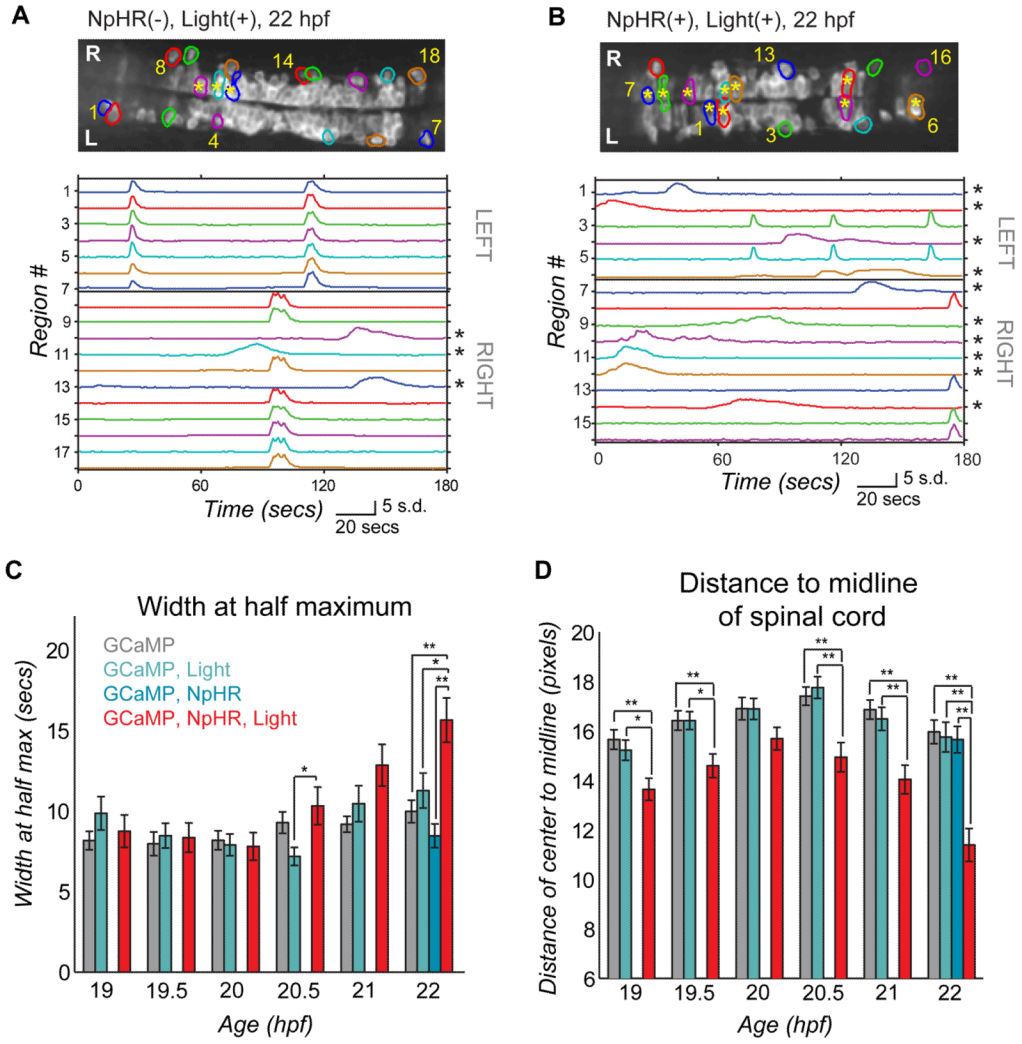

Figure 7. Light-inhibition decreases the number of cells joining the correlated network

(A,B) Baseline GCaMP fluorescence images with active regions circled (*top*, rostral left) and associated normalized intensity traces (*bottom*; amplitude plots standard deviation, s.d.) for example (A) control fish (without NpHR but illuminated with yellow/blue light protocol from 18–19 hpf) and (B) experimental fish (with NpHR and illuminated with yellow/blue light protocol from 18–19 hpf) at 22 hpf. Asterisks mark cells with long-duration, uncorrelated events, which increase in number in the experimental fish (B, *bottom*), and can be seen to reside in the medial spinal cord (b, *top*). (C) Average event duration through development was quantified using width at half maximum for experimental fish expressing NpHR and receiving the yellow light protocol (GCaMP, NpHR, Light) and for the three sets of control fish: i) lacking light and NpHR expression (GCaMP), ii) lacking NpHR expression (GCaMP, Light) or lacking light (GCaMP, NpHR). There was no difference between groups at 19, 19.5 20 and 21 hpf (one-way ANOVA at each time point, $P>0.05$), with significant differences at 20.5 and 22 hpf (one-way ANOVA at each time point, $P<0.05$), when experimental fish showed increases in event duration. (D) The distance from the cell center to the midline of the cord for active cells is reduced significantly in the experimental (GCaMP, NpHR, Light) fish compared to the three controls at all ages tested except for 20 hpf (one-way ANOVA at each time point, $P<0.05$). (C) and (D), means were calculated per cell (72–137 cells per group). Bars=s.e.m. Asterisks in (C) and (D) mark pair-

wise significance from post-hoc comparison with Bonferroni correction (* $P<0.05$; ** $P<0.01$). See also Supplemental Fig. 6.